

# MUON COLLECTION CHANNEL SIMULATIONS\*

D. Neuffer<sup>#</sup> and A. Van Ginneken, FNAL, Batavia, IL

## Abstract

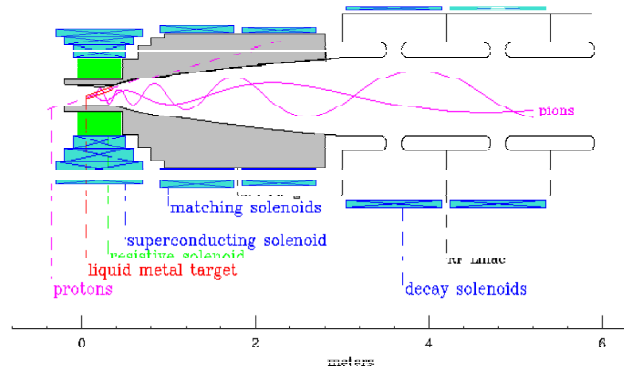
Results of Monte Carlo simulations of the processes in a collection channel for a muon collider are presented. In the simulations, pions are produced in a target, captured and then transported within solenoid focusing systems where they decay into muons. Muon yield and phase space characteristics at the end of the channel can be improved by placing rf cavities and absorbers along the channel as well as by providing a supplemental toroidal field along with the absorbers. Results for a sample of such scenarios are presented.

## 1 INTRODUCTION

A key requirement for a  $\mu^+\mu^-$  collider is to capture and collect a maximal number of muons from the proton source. For this, the proton beam from the source must be optimally focused onto a production target and the beam optics must be arranged to capture the maximal number of  $\pi$ 's and confine them within a transport channel for  $\pi \rightarrow \mu$  decay. A number of options for the target, the  $\pi$ -capture optics, and the  $\pi \rightarrow \mu$  decay transports have been studied.[1,2] From these studies it appears that an optimum scenario for producing forward  $\pi$ 's for  $\mu$ -collection is to use a high power 10–30 GeV proton beam which is focused onto a relatively high-Z, high-density target. The target is immersed in a high-field solenoid (20T in these studies) designed to capture  $\pi$ 's with transverse momentum up to 250 MeV/c. The captured  $\pi$ 's continue downstream from the target in a high-acceptance transport, which is based on solenoidal focusing with a low-frequency rf-bunching system, designed to capture the  $\mu$ 's from  $\pi$ -decay. Fig. 1 shows an overview of the target and initial portion of the collection and capture section, including the production target within a high-field capture solenoid and the transition into a lower-field solenoidal transport with a low-frequency rf system for capture and rotation.

In this transport the  $\pi$ 's decay into muons ( $\pi \rightarrow \mu\nu$ ) and the design problem is to optimize this transport to accept the maximum number of  $\mu$ 's, to capture them within a minimal phase-space volume, and transport them into an ionization cooling section. In this paper we explore several variations on designs for this capture section, including the possibility of providing some initial cooling in this section. (Much of this material is presented in more detail in ref. 4.)

**Figure 1:** Overview of the targetry + initial capture section of the  $\pi \rightarrow \mu$  collection channel.



## 2 CAPTURE AND COLLECTION SCENARIOS

The key parameters of the capture and cooling section (in the baseline design of solenoidal focusing plus rf capture) are the focusing field, the apertures, and rf parameters including rf voltage, frequencies, and phases.

In the simulations,  $\pi$  production is generated using the MARS code.[4] The 16 GeV proton beam ( $\sigma_x, \sigma_y = 0.4\text{cm}$ ) and bunch length of 0.3m (rms) is incident on a 36cm long, 1cm radius Ga target, situated in a 20T, 7.5cm radius, solenoid, and the simulations track the secondary particles from that source. The  $\pi$  trajectories initiate as helices in the 20T field. This field is adiabatically reduced in a transition solenoid to a smaller value which is sustained throughout the remaining transport/rf section. Final values of 5T and 1.25T are considered in the present simulations, some of which are presented in more detail in ref. [4]. In the adiabatic field decrease the radius of the transport channel is increased, keeping  $B r^2$  constant, to 15 cm with 5T and 30 cm with 1.25 T.

These studies of the capture and rf rotation process are based on previous studies by H. Kirk, R. Palmer and others, presented in ref. 1. Simulations by Palmer and Gallardo[5], by Y. Fukui[6], and the present studies, obtain  $\sim 0.2 \mu/p$  from the rf capture section with 16 GeV protons. Table 1 shows parameters of such a system. Our simulations show that at the end of the 42m rf rotation system  $\sim 0.22 \mu/p$  are captured within the  $r=15\text{cm}$   $B=5\text{T}$  transport, within an acceptance window of  $p=275 \pm 125 \text{ MeV/c}$ . The rms normalized emittance is 0.018 mrad, and  $\sigma_p \cong 50 \text{ MeV/c}$ ,  $\sigma_{ct} = 1.9\text{m}$ .

\*Research supported by DOE contract DE-AC02-76CH03000.

<sup>#</sup> Email: neuffer@fnal.gov

**Table 1:** parameters of an rf rotation/capture system for capture of  $\mu$ 's from  $\pi \rightarrow \mu\nu$  decay

Section	Length (m)	Rf frequency (MHz)	V'(rf) MV/m
1	6	90	5.2
2	18	50	3.15
3	18	30	2.1

This beam, however, has a large size (x, y, and z), and a large momentum spread at a relatively small momentum, and it is difficult to match into a following cooling and capture transport system.

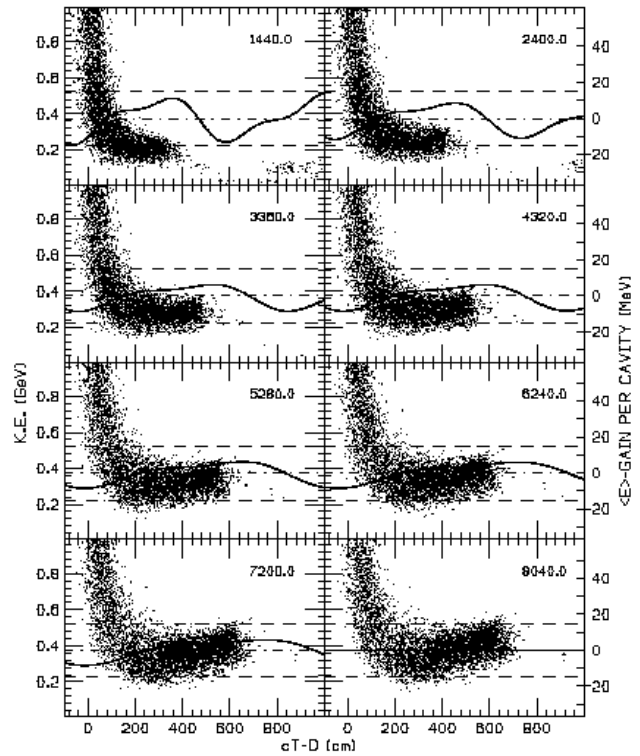
Based on these earlier studies and with some reoptimization a somewhat different capture scenario is developed, with parameters displayed in Table 2. This section is designed to capture the maximum number of muons from a target within a compressed bunch, using the large-aperture solenoid for transverse focusing, and an rf system for capturing and compressing the beam. The beam is significantly accelerated in preparation for subsequent cooling and capture transports. The bunch length/energy spread criterion used is an acceptance aperture of  $\pm 3\text{m}$  in longitudinal position and  $\pm 150\text{ MeV}$  in energy.

As shown in Table 2, the initial bunching is at higher rf frequencies, and the rf frequency decreases as the bunch travels downstream. rf voltages also decrease, since high-gradient is more difficult at lower frequencies. A double-frequency rf system is used throughout; the initial 90MHz rf voltage is supplemented by a double harmonic (180MHz) at 1/3 voltage. The double harmonic rf format improved capture from that obtained with single harmonic systems. The rf waveform is designed to decelerate the high energy end of the beam while accelerating the low energy end, reducing the energy spread with some increase in bunch length. In Fig. 2, the evolution of the bunch along the channel is displayed. The rf waveform in each section is also displayed, illustrating the bunch-rotation rf. The rf capture system is designed to accelerate the average beam energy to  $\sim 450\text{ MeV}/c$ , in order to prepare the beam for subsequent cooling.

**Table 2:** Parameters of an rf capture system and initial acceleration system. The rf system is double-harmonic, with an additional component at  $2\times$  the fundamental frequency and  $1/3$  the voltage, phase shifted by 2.2 radians.

Section	Length (m)	Fundamental rf frequency (MHz)	V'(rf) MV/m (fundamental)
1	7.2	90 $\rightarrow$ 60	13.5 $\rightarrow$ 11.7
2	7.2	54 $\rightarrow$ 44	10.8 $\rightarrow$ 9.0
3	19.2	42 $\rightarrow$ 34	8.55 $\rightarrow$ 5.85
4	24	33.5 $\rightarrow$ 26	5.4
5	24	25	5.4

**Figure 2:** Simulations of rf rotation in a 80m long, 5T solenoid channel, with the rf bunching systems of Table 1. The bunching wave form is shown as a line in each graph, which display the beam at regular intervals along the 80.4m transport, distance in cm is shown in each graph.



### 3 COOLING IN CAPTURE SCENARIOS

To explore the initiation of cooling within the  $\mu$ -collection system, an ionization cooling channel is added to the end of the rf rotation section, within the same transport. For ionization cooling, 0.1m long sections of LiH absorbers ( $\rho=0.82\text{ gm/cm}^3$ ,  $dE/dx = 1.56\text{ MeV/cm}$ ) are placed every 1.2m in a 72m long additional section. The rf acceleration is increased by  $\sim 15\text{ MV/m}$  to compensate for the beam energy losses in the absorbers. Simulations show that the system cooled transverse emittances by  $\sim 2\times$  and 6D emittance by  $\sim 4\times$  for the 5T case. (see Table 3) However the system heats the beam in the 1.25T case, causing large beam loss. The heating is caused by multiple scattering heating, which is  $4\times$  larger for that case, because of the weaker focusing. Adding toroidal magnets for additional focusing reduces the heating effect.

While these simulations show significant cooling, the system needs further development to be realized in practice. The rf gradients required are large for this frequency. The focusing system, even with an added toroidal field, is weaker than desired to suppress multiple scattering. Also some energy cooling is needed. Other systems, such as the alternating solenoid system presented in ref. [2], with emittance exchange cooling, should be developed and compared with this system.

The simulations do show that, from an initial production system, as many as 0.35  $\mu/p$  can be captured from a 16 GeV proton beam, which initially produces  $\sim 1.1 \pi/p$  at the target. An initial transverse cooling system within the solenoid channel can reduce beam sizes by a factor of two, which could make transfer from the rf rotation solenoid to a further cooling system much easier. Somewhat better capture is obtained using the stronger-focusing 5T lattice than the larger-aperture 1.25T case, and the more compact beam size is better suited for matching into downstream cooling sections.

Further modifications could make the system more practical and/or affordable. The many continuously-changing double-harmonic systems could probably be reduced to a few (i. e., 90, 60, 30) with little loss in performance. The initial cooling system could be modified to decelerate the beam with cooling, which may be more efficient, and alternating-solenoid focusing could replace the toroids in focusing the beam. Deceleration would reduce rf requirements; our initial scenario actually accelerates the beam. However, more reacceleration in cooling segments would be needed. A sparser absorber configuration (possibly using  $H_2$  absorbers as in ref. 2) would reduce gradient requirements, while lengthening the system. Some energy cooling in this initial stage is desirable.

#### 4 DISCUSSION: FUTURE STUDIES

The chief difficulty which needs further study is the problem of matching the very large beam from the rf rotation channel into a following cooling channel. At that point the beam has an rms  $\delta p/p$  of  $\sim 15\%$ , a bunch length of  $\sim 1.4m$  rms (6m full width), and transverse beam sizes of  $\sim 7cm$  radius (15 cm full radius) with an angular width of 100 mrad. The general technique of inserting some initial cooling within the rf rotation channel will probably be used, and both transverse cooling and emittance-exchange components are needed. An important challenge which needs a specific solution is the design of a first energy-cooling (emittance-exchange) system which can accommodate the very large emittances and momentum spreads at the end of the rf rotation channel, with minimal dilution and losses.

#### 5 REFERENCES

[1]  $\mu^+\mu^-$  Collider: A Feasibility Study, BNL-52503, FNAL-Conf-96/692, LBNL-38946, presented at Snowmass 1996.  
 [2] C. M. Ankenbrandt et al., *Status of Muon Collider Research and Development and Future Plans*, BNL-65623, Fermilab-PUB-98/179, LBNL-41935, to be published in Phys. Rev. Spec. Topics AB (1999)  
 [3] A. Van Ginneken and D. Neuffer, Fermilab-Pub-98/296(1998), to be published in Nucl. Inst. and Meth. A (1999)  
 [4] N.V. Mokhov, *The MARS Code System Users Guide*, FNAL-FN-628 (1995), MARS files provided by N.V. Mokhov.  
 [5] R. Palmer and J. Gallardo, MCMuon simulation results, unpublished (1998).  
 [6] Y. Fukui, unpublished (1998).

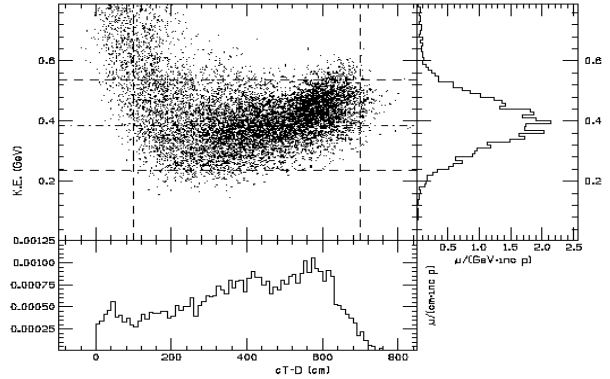


**Figure 3:** Longitudinal profiles of the beam at the end of the rf capture sequence, but before any cooling.

**Table 3:** Results of simulations of rf rotation scenarios for 5T and 1.25T focusing systems. In the second column cooling absorbers are added, and an additional focusing field is added in the third column.

$R_{sol}, cm/B_{sol}, T$	no absorbers		absorbers		+toroidal field	
	15/5	30/1.25	15/5	30/1.25	15/5	30/1.25
$N_{\mu}$	0.349	0.287	0.302	0.130	0.324	0.258
$\epsilon_6, cm^2$	225	257	63	271	63	153
$\langle \epsilon_T^2 \rangle^{1/2}, cm$	1.63	1.73	0.91	1.81	0.86	1.36
$\epsilon_{z1}, cm$	2.18	2.08	0.92	2.11	0.89	1.37
$\langle \sigma^2 \rangle^{1/2}, cm$	4.85	10.12	4.45	11.17	3.06	5.02
$\sigma_E, MeV$	72	78	68	62	72	61
$\langle E_{kin} \rangle, MeV$	350	307	407	475	480	484
$N_{\mu}^2/\sqrt{\epsilon_6}, cm^{-3/2}$	0.0081	0.0051	0.0115	0.0010	0.0132	0.0054